INTERNATIONAL JOURNAL OF AGRICULTURE & BIOLOGY
ISSN Print: 1560–8530; ISSN Online: 1814–9596
18–0307/201x/00–0–000–000
DOI: 10.17957/IJAB/15.0767
http://www.fspublishers.org

Short Communication

Antifungal Effect of *Buxus sinica* Leaf Extract-mediated Silver Nanoparticles against *Curvularia lunata*

Weidong Huang, Huizhong Li, Haiming Duan, Yaling Bi, Degong Wu, Junli Du and Haibing Yu*
College of Agriculture, Anhui Science and Technology University, Fengyang 233100, China
*For correspondence: haibing50721@163.com

Abstract

Buxus sinica leaf extract was used to synthesize silver nanoparticles, and leaf extract volume, concentration of $AgNO_3$, and pH value were adjusted to ascertain the optimized biosynthesis system, it included 20 mL of leaf extract, 4 m*M* $AgNO_3$, and pH of 7. Transmission Electron Microscopy (TEM) images revealed that the silver nanoparticles were spherical and finely dispersed, with an average size of 5.6 nm. SEM (Scanning Electronic Microscopy) and EDX (Energy-dispersive X-ray) further confirmed their morphology and purity. As-synthesized silver nanoparticles exhibited prominent antifungal activity against *Curvularia lunata*. At a dose of 200 μg mL^{-1} of silver nanoparticles, the inhibition rate of colony growth reached 85% and an IC_{50} value of 26 μg mL^{-1}. Furthermore, an inhibition of 100% conidial germination and IC_{50} of 9.16 μg mL^{-1} were achieved at 50 μg mL^{-1}. Silver nanoparticles exerted destructive effects on mycelial morphology, which became expanded and distorted. The silver nanoparticles effectively prevented the germination of and infection by conidia of *C. lunata*. It is possible to screen silver nanoparticles as one kind of high efficient fungistatic agent to assist or replace chemical pesticide. © 2018 Friends Science Publishers

Keywords: Silver nanoparticles; Inhibition rate; Optimized biosynthesis

Introduction

Silver has been applied to diminish inflammation and heal wounds since ancient times owing to its broad spectrum of antimicrobial effects. Unlike other metals, silver exhibits higher toxicity to microorganisms, such as bacteria, fungi, and viruses, while presenting lower toxicity to mammalian cells (Li *et al.*, 2010). Nowadays, traditional silver compounds are produced at the nanoscale by using nanotechnology. The nanoparticles have unique optical, physical, chemical, and magnetic properties (You *et al.*, 2012). Silver nanoparticles have shown wide prospects for application in many fields, including medicine, electronics, cosmetics, water disinfection, etc. (Zhao *et al*., 2011; Bakshi *et al*., 2014).

In recent years, the synthesis, characterization, and application of silver nanoparticles have attracted increasing research attention. Silver nanoparticles could be synthesized through physical, chemical, and biological methods. For example, physical methods utilize high temperature and high pressure, and require performing complicated operations (Yin *et al.*, 2004; Nadagouda *et al*., 2011). Although the chemical method is easy to apply, toxic reagents such as reducing and stabilizing agents, and organic solvents with potential environmental contamination risks are required for its utilization (Albrecht *et al.*, 2006; Song *et al.*, 2009). The idea of green chemistry has prompted considerable scientific focus on methods based on biosynthesis by microorganisms and plant tissues (Huang *et al.*, 2013; Narayanan and Park, 2014; Khatami and Pourseyedi, 2015; Khatami *et al.*, 2016). Unlike physical and chemical methods, the biosynthesis method is considered an environmentally friendly approach with several advantages, including low cost, adequate stability, minimal use of toxic reagents, and thus greater environmental safety, etc.

Pathogen prevention in the medical and agricultural domains is a persistent issue, which is even more difficult to deal with due to the current situation of climatic changes and pathogenic variability. It is necessary to establish the neotype and discover novel efficient antimicrobial substances that assist or replace traditional reagents. As a non-antibiotic substance, biosynthesized silver nanoparticles exhibit excellent antimicrobial properties against human, animal, and plant pathogens (Schluesener and Schluesener, 2013; Hussain *et al.*, 2016). Silver nanoparticles have been used to inhibit the development of phytopathogens a few years ago, but the research is still at its initial stage.

In this report, the antifungal activity of *Buxus sinica* leaf extract-mediated silver nanoparticles against *Curvularia lunata* was determined. To our knowledge, this is the first report showing effective antifungal control exerted by optimized *B. sinica* based silver nanoparticles.

To cite this paper: Huang, W., H. Li, H. Duan, Y. Bi, D. Wu, J. Du and H. Yu, 201x. Antifungal effect of *buxus sinica* leaf extract-mediated silver nanoparticles against *curvularia lunata*. *Int. J. Agric. Biol*., 00: 000–000

The major objectives of this study included exploration of the optimal system conditions for the biosynthesis of silver nanoparticles, as well as evaluation of the efficacy and potency of *B. sinica*-mediated silver nanoparticles against *C. lunata*. These findings can be used either alone or for application of these nanoparticles in combinations with other chemical reagents for the control of Curvularia leaf spot of maize.

Materials and Methods

Preparation of Leaf Extract

The extract of *B. sinica* was prepared as follows. Leaves were washed in sterile water several times and cut into small pieces (1 cm × 1 cm), followed by air-drying on a clean bench. An amount of 10 g of the above cut leaves was added to 100 mL of deionized water and heated at 95°C for 30 min. During the heating process, intermittent stirring was performed to achieve uniform heating. Then, the extract was filtered through filter paper and preserved at 4°C for further experiments.

Optimized Biosynthesis of Silver Nanoparticles

Silver nanoparticles were biosynthesized by addition of the leaf extract to deionized water at a ratio of 1:9 (v:v), followed by reaction with $AgNO_3$ at a temperature of lower than 60°C. An optimization process was performed, including the examination of different volumes of the leaf extract (5, 10, 20, and 50 mL), concentrations of $AgNO_3$ (1, 2, 4, and 8 m*M*), and pH values (pH 3, 5, 7, 9 and 11).

Characterization of Silver Nanoparticles

Obvious solution color change was observed after incubation for 15 min. The formation of silver nanoparticles was determined by UV-Vis spectroscopy (TU-1950, PERSEE, China). TEM (JEM-2100F, JEOL, Japan) and field-emission SEM (S-4800, Hitachi, Japan) were also performed, and the purity of silver nanoparticles was measured by energy-dispersive X-ray analysis (EDX).

Antifungal Activity of Silver Nanoparticles against *C. lunata*

Inhibition of colony growth: Oven-dried silver nanoparticles were dissolved in sterile water as a stock solution (10 mg mL^{-1}). A volume of 5 mL of diluted stock solution was added to 45 mL of PDA (Potato Dextrose Agar) medium at an approximate temperature of 55-60°C, and final concentrations of silver nanoparticles of 6.25, 12.5, 25, 50, 100, and 200 μg mL^{-1}were obtained by dilution with sterile water. The control set contained 5 mL of sterile water without silver nanoparticles. A fungus block (φ=5 mm) was inoculated in the center of each Petri dish containing a different concentration of silver nanoparticles, followed by incubation at 28°C for 3-5 d. Each control and experimental treatment was performed in three replicates.

Influence on Conidia Germination

The densities of *C. lunata* conidia were adjusted to 10^6 mL^{-1} by a counting chamber. Next, various concentrations of silver nanoparticles (6.25, 12.5, 25, 50, 100 and 200 μg mL^{-1}) and conidia suspensions were added into sterile centrifuge tubes at a ratio of 1:9 (v: v). The conidia suspension served as control. Then, incubation at 25°C for 1-2 d was performed. Images of conidia in the control and experimental treatments were obtained under a microscope (100 X).

Influence on Mycelial Morphology

Mycelia were treated with different concentrations of silver nanoparticles (6.25, 12.5, 25, 50, 100 and 200 μg mL^{-1}), followed by incubation at 25°C for 2-3 d. Mycelial solution with sterile water served as control. The morphology of the mycelia in the control and experimental treatments were photographed under a microscope (400 X).

Detached Leaf Assay

Maize leaves (Zhengdan 958, ZD958) were washed thoroughly with sterile water, surface-sterilized by dipping into 2% (v/v) sodium hypochlorite for 1 min, and rinsed three times with sterile water under aseptic conditions. Air-dried leaves were placed in a sterile Petri dish containing PDA medium and inoculated with 10 μL of the solutions with different concentrations of silver nanoparticles (6.25, 12.5, 25, 50, 100 and 200 μg mL^{-1}). A suspension of leaves spotted with conidia served as control; four drops per leaf, and four replicates for each treatment were applied.

Results

Biosynthesis of Silver Nanoparticles

$AgNO_3$ (Ag^+) was reduced into metallic silver (Ag^0) in the presence of the plant extract, and the solution color changed from light green (Fig. 1b) to red brown (Fig. 1c), while the $AgNO_3$ solution without the plant extract remained colorless (Fig. 1a). The solution color change indicated formation of silver nanoparticles. The UV-Vis absorption spectrum showed a sharp absorbance at 448 nm, corresponding to the surface plasmon resonance of silver nanoparticles (Shukla *et al.*, 2012). However, there was no obvious absorption peak for the $AgNO_3$ solution and *B. sinica* leaf extract (Fig. 1d).

Construction of an Optimal Biosynthesis System

Effect of plant extract volume: The plant extract volume had a direct relation to its reducing action. Under the same condition of 1 m*M* $AgNO_3$, the solution color darkened with the increase in volume (Fig. 2a).

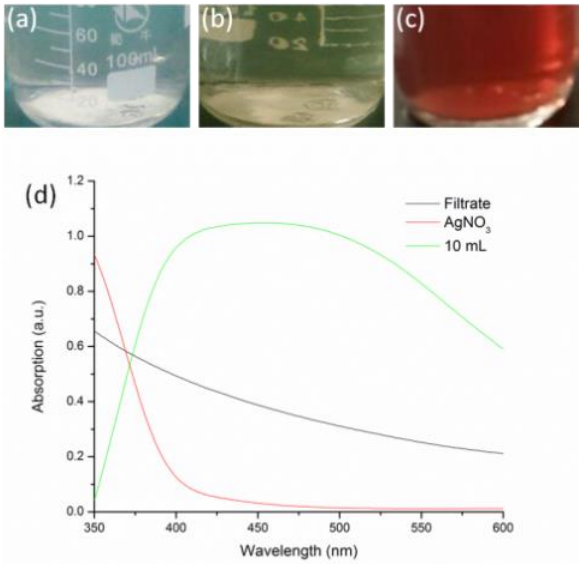

Fig. 1: Biosynthesis of silver nanoparticles based on 10 mL of *B. sinica* leaf extract. (a) $AgNO_3$ solution; (b) leaf extract; (c) leaf extract with 1 mM $AgNO_3$; (d) Corresponding UV-Vis absorption spectra

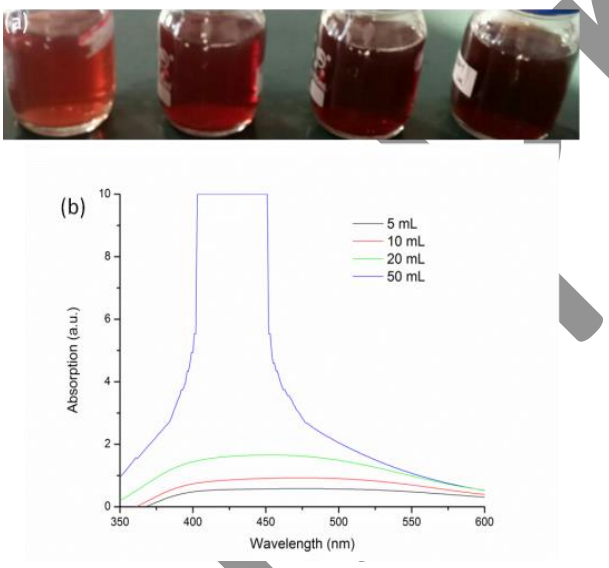

Fig. 2: Effect of the varied volume of *B. sinica* leaf extract on silver nanoparticles formation. (a) Photograph of silver nanoparticles based on 5, 10, 20, and 50 mL of *B. sinica* leaf extract (from left to right); (b) Corresponding UV-Vis absorption spectra

UV-Vis spectra showed that the maximum absorption was gradually elevated from 5 mL to 50 mL (Fig. 2b). While the spectrum of solution based on 50 mL filtrate exceeded the acceptable range (higher than 9.99) and was prone to aggregation; thus, the optimal plant extract volume was determined as 20 mL.

Effect of Varied Concentrations of $AgNO_3$

The concentration of $AgNO_3$ had a direct relation to the content of the synthesized silver nanoparticles. The solution color turned from red-brown to black-brown as the concentration of $AgNO_3$ increased from 1 m*M* to 8 m*M* (Fig. 3a). UV-Vis spectra showed that the absorption peak increased gradually with the augmentation of the concentration of $AgNO_3$ and reached its maximum at 4 m*M* $AgNO_3$ (Fig. 3b). Hence, the optimum concentration of $AgNO_3$ was determined as 4 m*M*.

Effect of Varied pH

Solution pH is an important factor that affects the formation, size, and morphology of silver nanoparticles. As shown in Fig. 4a, solutions with varied pH (3, 5, 7, 9 and 11) presented a different color. At pH 3 and 5, the solution was milk-white and yellow-orange, respectively, and its UV-Vis absorption spectra (Fig. 4b, black and red curves) did not correspond to the surface plasmon resonance of the silver nanoparticles. At pH 7–11, the solution color turned from red-brown to black-brown, while the spectra of solution at pH 9 and 11 exceeded the acceptable range (higher than 9.99), which might cause instability; thus, the optimal pH value was determined as 7.

Characterization of Silver Nanoparticles

TEM analysis: As can be seen in the TEM image in Fig. 5, the synthesized silver nanoparticles were typically spherical or near spherical with favorable dispersal behavior (Fig. 5a). To determine the particle size and size distribution, 200 particles were randomly selected from several TEM images. The size of the biosynthesized silver nanoparticles was found to be in the range 2.6~10.8 nm, and the average particle size was approximately 5.6 nm (Fig. 5b).

SEM and EDX analysis: The SEM image in Fig. 6a displays synthesized silver nanoparticles with a spherical shape. As can be observed in the EDX spectrum of silver nanoparticles in Fig. 6b, the peaks around 3 Kev indicate the existence of elemental silver, signal of Pt owing to gold film coated on sample before scanning, while other peaks like Cl, Al, C, O, and Si should be due to components of *B. sinica* leaf extract and other solutions.

Inhibition of Colony Growth

As shown in Fig. 7, silver nanoparticles exhibited a prominent inhibition effect on colony growth. The diameter of *C. lunata* without silver nanoparticles measured by cross method was 6.73 cm (Fig. 7a), and it decreased gradually with the rise in the concentration of silver nanoparticles (Fig. 7b, c, d, e, f and g). The diameter of the silver nanoparticles reached its minimum value (1.43 cm) at 200 μg mL^{-1} (Fig. 7g).

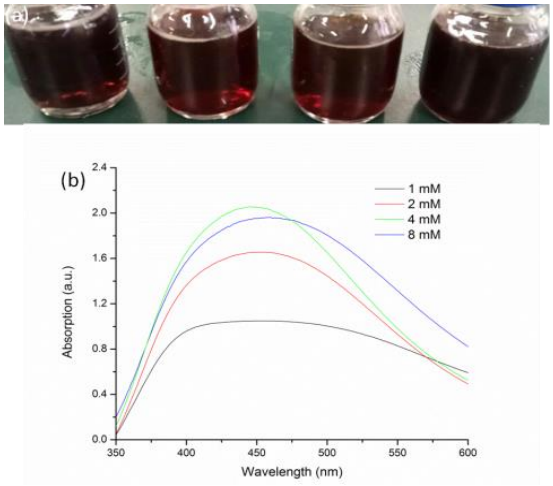

Fig. 3: Effect of varied concentrations of $AgNO_3$ on silver nanoparticles formation. (a) Photograph of silver nanoparticles based on 1, 2, 4 and 8 mM $AgNO_3$ (from left to right); (b) Corresponding UV-Vis absorption spectra

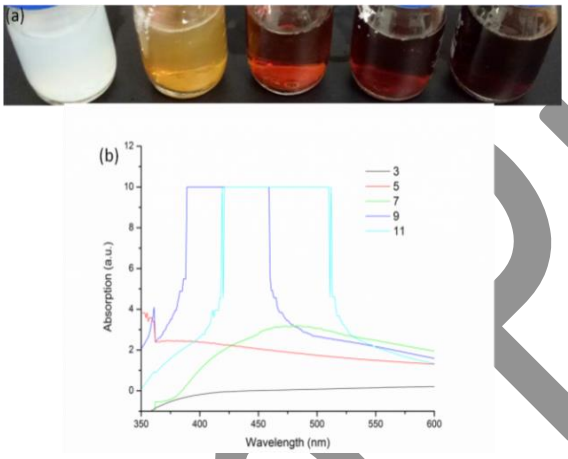

Fig. 4: Effect of varied pH on silver nanoparticles formation. (a) Photograph of silver nanoparticles with pH 3, 5, 7, 9 and 11 (from left to right); (b) Corresponding UV-Vis absorption spectra

The data from three replicates of the treatments with different concentrations were averaged and used to calculate by SPSS 13.0 the median inhibitory concentration (IC_{50}), which was 26.06 μg mL^{-1} (95% CI: 15.18-40.68 μg mL^{-1}). The inhibition rate caused by the varied silver nanoparticles concentrations (6.25-200 μg mL^{-1}) in the control and experimental treatments of *C. lunata* was in the range 8.99%-85.07%.

Influence of Conidia Germination

As seen from the data in Table 1, silver nanoparticles affected dramatically the germination of conidia of *C. lunata*. In the control, the germination rate was 91.67%, but it decreased

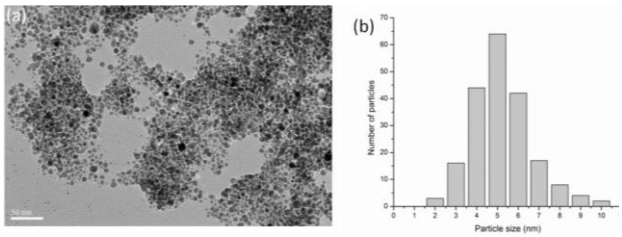

Fig. 5: TEM image (a) and size distribution (b) of silver nanoparticles

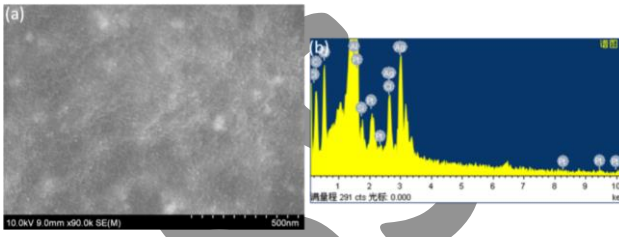

Fig. 6: SEM image (a) and EDX spectrum (b) of silver nanoparticles

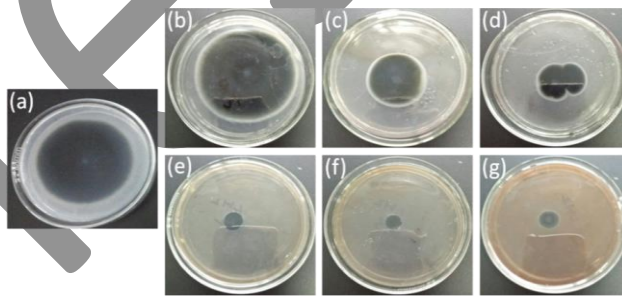

Fig. 7: Inhibition of the colony growth of *C. lunata* by silver nanoparticles. (a) colony of the control isolate; (b)-(g), *C. lunata* with silver nanoparticles concentration of 6.25, 12.5, 25, 50, 100 and 200 μg mL^{-1}

obviously with the increase in the concentration of silver nanoparticles, and conidia were totally inhibited at 50 μg mL^{-1} or more. IC_{50} calculated by SPSS 13.0 was 9.16 μg mL^{-1} (95% CI: 8.42–9.88 μg mL^{-1}).

Influence on Mycelial Morphology

Mycelia of *C. lunata* treated with silver nanoparticles had abnormal morphology. As shown in Fig. 8, the mycelia of the control isolate were intact, smooth, and well-organized (Fig. 8a), whereas the incubation with silver nanoparticles (200 μg mL^{-1}) for 3 d caused breakdown of mycelia to fragments (Fig. 8b), surface roughening, expansion (Fig. 8c), and multiangular distortion (Fig. 8d).

Detached Leaf Assay

C. lunata causes a serious foliar spot disease in maize leading to major yield losses. The process of infection starts with

Table 1: Influence of silver nanoparticles on conidia germination of *C. lunata*

Concentration (μg.mL^{-1})	Total number of conidia	Number of germinated conidia	Germination rate (%)	Inhibition rate (%)
0	300	275	91.67	--
6.25	300	192	64.00	30.18
12.5	300	91	30.33	66.91
25	300	28	9.33	89.82
50	300	0	0	100
100	300	0	0	100
200	300	0	0	100

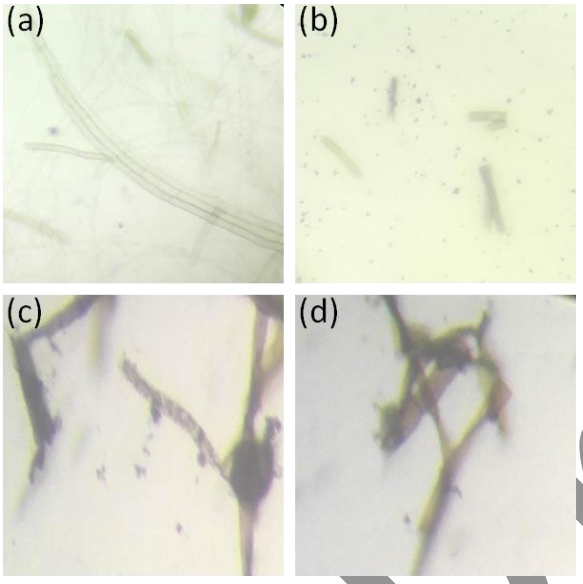

Fig. 8: Influence of silver nanoparticles on the mycelial morphology of *C. lunata*. (a), mycelia of control isolate; (b)–(d), mycelia treated with silver nanoparticles

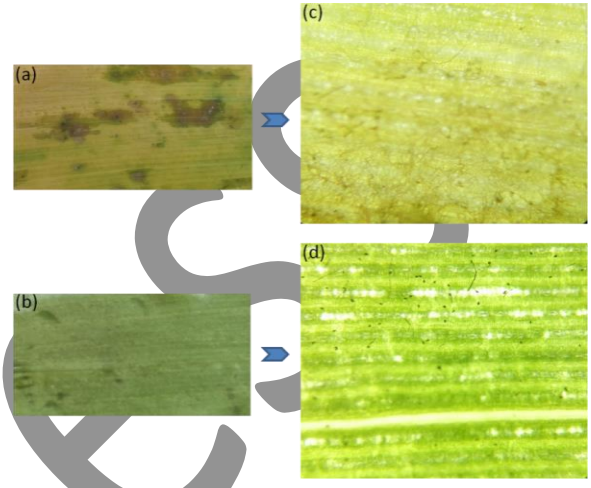

Fig. 9: Detached leaf assay of the use of silver nanoparticles against *C. lunata*. (a) maize leaf inoculated with a conidia suspension of *C. lunata*; (b) maize leaf inoculated with a conidia suspension of *C. lunata* and silver nanoparticles; (c) microscopic image of the local area of (a); (d) microscopic image of the local area of (b)

conidia germination on the leaf surface, and thus it is the key point that determines whether a disease would occur. Maize leaves inoculated with a conidia suspension of *C. lunata* alone for 3 d showed obvious disease symptoms, and the leaves turned yellow (Fig. 9a). Conversely, the combination of conidia suspension and silver nanoparticles reduced significantly disease severity. Especially when the concentration of silver nanoparticles was 200 μg mL^{-1}, no spot blotch appeared on the treated maize leaves, and they looked as healthy as the control leaves (Fig. 9b). Microscopic images further confirmed the complete conidia germination on maize leaves inoculated with *C. lunata* alone (Fig. 9c), which was totally inhibited by the treatment with silver nanoparticles (Fig. 9d).

Discussion

Synthesis and application of silver nanoparticles is a prevalent field in view of their distinct characteristics. In the past few years, biosynthesis of silver nanoparticles by plant tissues has been reported (Borase *et al.*, 2014; Roy and Das, 2015; Abdelghany *et al.*, 2018), as far as we know, *B. sinica* has not been applied for this purpose, and few reports focused on optimized biosynthesis (Krishnaraj *et al.*, 2012; Iravani and Zolfaghari, 2013). In addition, solution color change and UV-Vis absorption spectra were integrated to ascertain the optimal synthesis conditions based on selected plant tissues. The attempts for prevention and control of *C. lunata*, a worldwide plant pathogen on maize, have never ceased. However, the application of nanoparticles especially metal nanoparticles against phytopathogen is a newly developed field. Introduction of such materials into plant disease control could reduce its long-term dependence on chemical pesticides, and contribute to resolve some problems like environment pollution, pesticide residue, fungicides resistance, etc. Although silver nanoparticles synthesized by *Acalypha indica* leaf extract were used to inhibit *C. lunata* in a previous examination (Krishnaraj *et al.*, 2012), the effective inhibition concentration was 0.5 mg μL^{-1}, which is more than ten thousand times the concentration (50 μg mL^{-1}) selected here that totally inhibited conidia germination. It is supposed that the size, morphology, dispersity, and purity of silver nanoparticles might be directly associated with their antimicrobial activity (Ivask *et al.*, 2014). Our results indicated that such synthesized silver nanoparticles exhibit prominent antifungal activity against *C. lunata*,

and the potential of an environmentally friendly inhibitory substance was screened for comprehensive management of phytopathogens.

Conclusion

On the basis of these results, silver nanoparticles were biosynthesized by *B. sinica* leaf extract, and the optimal synthesis system was also ascertained through adjusting filtrate volume, AgNO3 concentration, and pH value. In addition, silver nanoparticles synthesized here show excellent antifungal activity against *C. lunata*. As one kind of non-antibiotic fungistat, silver nanoparticles could prevent the development of drug-resistant pathogens to the utmost extent. Further experiments should focus on parameters that influence their antifungal activity such as high temperature, ultraviolet ray, aggregation behavior, and surface charge, and so on.

Acknowledgements

This work was supported by the, Key Discipline of Plant Protection in University of Science and Technology of Anhui (AKZDXK2015C04), Natural Science Fund of Education Department of Anhui province (KJ2017A510), Talent introduction project in Anhui Science and Technology University (NXYJ201602), Innovation project of university students (201710879072).

References

Abdelghany, T.M., A.M.H. Al-Rajhi, M.A. Al-Abboud, M.M. Alawlaqi, A.G. Maqdah, E.A.M. Helmy and A.S. Mabrouk, 2018. Recent advances in green synthesis of silver nanoparticles and their applications: About future directions. *BioNanoSci*., 8: 5–16

Albrecht, M.A., C.W. Evan and C.L. Raston, 2006. Green chemistry and the health implications of nanoparticles. *Green Chem.*, 8: 417–432

Bakshi, M., H.B. Singh and P.C. Abhilash, 2014. The unseen impact of nanoparticles: More or less? *Curr. Sci.*, 106: 350–352

Borase, H.P., B.K. Salunke, R.B. Salunkhe, C.D. Patil, J.E. Hallsworth, B.S. Kim and S.V. Patil, 2014. Plant extract: a promising biomatrix for ecofriendly, controlled synthesis of silver nanoparticles. *Appl. Biochem. Biotechnol*., 173: 1–29

Huang, W.D., J.J. Yan, Y. Wang, C.L. Hou, T.C. Dai and Z.M. Wang, 2013. Biosynthesis of Silver Nanoparticles by *Septoria apii* and *Trichoderma koningii*. *Chin. J. Chem.*, 31: 529–533

Hussain, I., N.B. Singh, A. Singh, H. Singh and S.C. Singh, 2016. Green synthesis of nanoparticles and its potential application. *Biotechnol. Lett.*, 38: 545–560

Iravani, S. and B. Zolfaghari, 2013. Green synthesis of silver nanoparticles using Pinuseldarica bark extract. *BioMed Res. Int.*, 2013, DOI: 10.1155/2013/639725

Ivask, A., I. Kurvet, K. Kasemets, I. Blinova, V. Aruoja, S. Suppi, H. Vija, A. Kakinen, T. Titma, M. Heinlaan, M. Visnapuu, D. Koller, V. Kisand and A. Kahru, 2014. Size-dependent toxicity of silver nanoparticls to bacteria, yeast, algae, crustaceans and mammalian cells *in vitro*. *Plos One*, 9, DOI: 10.1371/journal.pone.0102108

Khatami, M. and S. Pourseyedi, 2015. *Phoenix dactylifera* (date palm) pit aqueous extract mediated novel route for synthesis high stable silver nanoparticles with high antifungal and antibacterial activity. *IET Nanobiotechnol*., 9: 184–190

Khatami, M., R. Mehnipor, M.H.S. Poor and G.S. Jouzani, 2016. Facile biosynthesis of silver nanoparticles using *Descurainiasophia* and evaluation of their antibacterial and antifungal properties. *J. Clust. Sci*., 27: 1601–1612

Krishnaraj, C., R. Ramachandran, K. Mohan and P.T. Kalaichelvan, 2012. Optimization for rapid synthesis of silver nanoparticles and its effect on phytopathogenic fungi. *Spectrochim. Acta A*, 93: 95–99

Li, W.R., X.B. Xie, Q.S. Shi, H.Y. Zeng, Y.S. Ou-Yang and Y.B. Chen, 2010. Antibacterial activity and mechanism of silver nanoparticles on *Escherichia coli*. *Appl. Microbiol. Biotechnol.*, 85: 1115–1122

Nadagouda, M.N., T.F.V. Speth and R.S. Varma, 2011. Microwave-Assisted Green Synthesis of Silver Nanostructures. *Accounts Chem. Res*., 44: 469–478

Narayanan, K.B. and H.H. vPark, 2014. Antifungal activity of silver nanoparticles synthesized using turnip leaf extract (*Brassica rapa* L.) against wood rotting pathogens. *Eur. J. Plant Pathol.*, 140: 185–192

Roy, S. and T.K. Das, 2015. Plant mediated green synthesis of silver nanoparticles-a review. *Int. J. Plant Biol. Res.*, 3: 1044–1054

Schluesener, J.K. and H.J. Schluesener, 2013. Nanosilver: application and novel aspects of toxicology. *Arch. Toxicol.*, 87: 569–576

Shukla, M.K., R.P. Singh, C.R.K. Reddy and B. Jha, 2012. Synthesis and characterization of agar-based silver nanoparticles and nanocomposite film with antibacterial applications. *Bioresour. Technol.*, 107: 295–300

Song, W.H., X.X. Zhang, H.Z. Yin, P.P. Sa and X.Y. Liu, 2009. Preparation and Storage of Silver Nanoparticles in Aqueons. *Chin. J. Chem.*, 27: 717–721

Yin, H., T. Yamamoto, Y. Wada and S. Yanagida, 2004. Large-scale and size-controlled synthesis of silver nanoparticles under microwave irradiation. *Mater. Chem. Phys.*, 83: 66–70

You, C., C. Han, X. Wang, Y. Zheng, Q. Li and X. Hu, 2012. The progress of silver nanoparticles in the antibacterial mechanism, clinical application and cytotoxicity. *Mol. Biol. Rep.*, 39: 9193–9201

Zhao, L., H. Wang, K. Huo, L. Cui, W. Zhang and H. Ni, 2011. Antibacterial nano-structured titania coating incorporated with silver nanoparticles. *Biomaterials*, 32: 5706–5716

(Received 28 February 2018; Accepted 22 May 2018)